

Modelling of trapped high density electron clouds relevant to gyrotrons

G. Le Bars¹, J.-P. Hogge¹, J. Loizu¹, S. Alberti¹, A. Cerfon²

¹ Ecole Polytechnique Fédérale de Lausanne (EPFL), Swiss Plasma Center (SPC), CH-1015 Lausanne, Switzerland

² New York University, Courant institute of mathematical sciences, NY-10012 New York, USA

Nonneutral plasmas are of broad interest for antimatter physics, particle accelerators and high power microwave sources such as gyrotrons. Indeed, the study of charged particle confinement is crucial for developing long-term antimatter storage (Penning traps) or to avoid arcing and improve efficiency of particle accelerators and microwave sources.

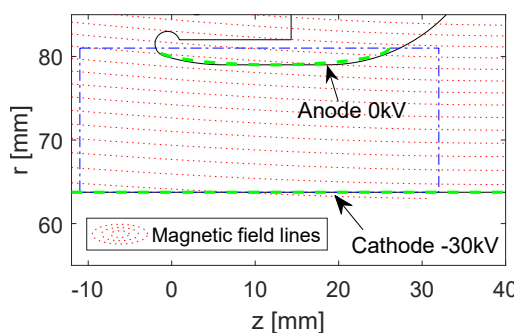


Figure 1: Black: geometry of the gt170 gyrotron gun assembly[1]. Green: approximated geometry used in simulations. Blue: simulation domain

In gyrotrons specifically, operation has been sometimes compromised by the presence of localized trapped electrons (i.e. not belonging to the main electron beam) in the gyrotron gun region [1]. Such trapped electrons can lead to arcing and, in some cases, prevent the electron gun from operating at nominal electron acceleration voltage [2]. The trapping of particles is due to the presence of crossed electric and magnetic fields and has some analogies to a Penning-Malmberg trap. Furthermore, the trapped electrons are believed to cause an increase of the cloud density by ionizing the residual neutral gas present in the vacuum vessel, eventually leading to a sudden release of charge by means of an as-of-yet unidentified instability. In fact, there is currently a lack of basic understanding of the trapped electron cloud dynamics and a general study is needed to pinpoint the physical parameters that determine the sudden loss of confinement resulting in arcing events observed experimentally.

Simulation model, geometry and source

To study this problem, a 2D electrostatic particle-in-cell code assuming azimuthal symmetry has been developed. This code solves the Vlasov-Poisson equation for the electrostatic potential Φ and the electron distribution function f by using a finite element method for Poisson and a Boris integrator for the particle pusher [3]. The

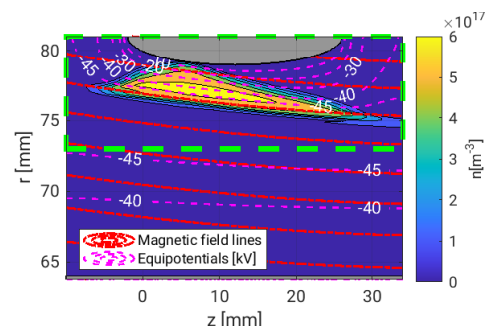


Figure 2: Steady state reached by the system when the electron source is activated. The green box represents the extent of the source.

simulations domain considered in this study is shown in Figure 1 (blue box) and the geometry of the electrodes in the simulations is an approximation of the complex electron gun geometry. To this end, a constant radius coaxial insert at -30kV is used for the cathode and an elliptic boundary for the anode at 0kV .

This leads to the following electric potential boundary conditions, imposed using weighted-extended b-splines [4]:

$$\Phi \Big|_{\text{cathode}} = \Phi_a, \Phi \Big|_{\text{anode}} = \Phi_b, \nabla \Phi \cdot \vec{n} \Big|_{\text{otherwise}} = 0. \quad (1)$$

This method allows the definition of Dirichlet boundary conditions on curved domains while keeping a rectangular grid which permits fast computations and a high flexibility for the geometry definition. For the particles, perfectly absorbing boundary conditions are imposed and an ad-hoc electron source is applied that coarsely emulates the electron creation by ionization of the residual neutral gas present in the vessel. This volumetric source creates electrons at a fixed rate using a uniform distribution in space and a Maxwellian distribution in velocity with a temperature of 1eV . Starting with an empty vessel and using this source, the system reaches a quasi-steady state that is represented in figure 2.

Simulation results

To understand this steady state, we performed parametric scans on the externally applied potential bias between the electrodes, the anode curvature radius and the magnetic field amplitude. For each of these cases we used the same volumetric source term and we looked at the cloud maximum density, height and the total number of electrons in the simulation in the steady-state regime. As can be seen on the results of figure 3, the anode curvature radius has a low impact, the potential bias has a medium impact and the

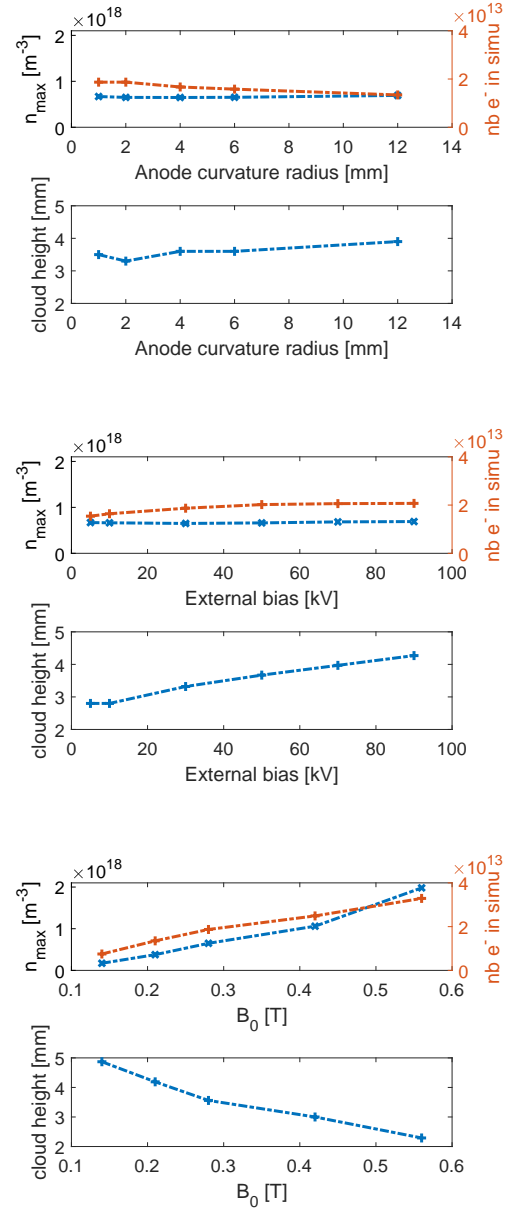


Figure 3: Maximum density in the cloud, number of electrons in the simulation and cloud height obtained at steady state for different values of the scanned parameters.

magnetic field amplitude has a strong impact on the confinement. These last two parameters could then be used to control the cloud density.

Diocotron instability study

Non-neutral plasmas in the presence of a magnetic field are susceptible to the diocotron instability which grows with azimuthal wavelengths and is similar in nature to the Kelvin-Helmholtz instability.

It arises due to radial shear in the azimuthal velocity and, because our PIC code does not simulate the dynamics in this direction, we perform a linear instability study a posteriori using the steady-state density profiles. To calculate the linear stability to diocotron normal modes, we use an electrostatic eigenvalue equation derived using the electrostatic fluid model, assuming low-density ($\omega_{pe}^2/\omega_{ce}^2 \ll 1$) and in the non-inertial limit (massless electrons) [5, 6]. This model considers an infinite length annular electron cloud trapped radially by a strong uniform magnetic field. A metallic conductor is present at radial

position b and a coaxial insert at a can be added with a given bias between the conductors. In this model, the electrostatic potential is described as an equilibrium term plus a linear normal mode perturbation:

$$\phi = \phi_0 + \sum_{l=-\infty}^{\infty} \delta\phi^l(r) \exp(il\theta - i\omega t), \quad (2)$$

and similarly for the density. Combining the force balance, continuity and Poisson equations, the following eigenvalue equation is obtained [6]:

$$\frac{1}{r} \frac{\partial}{\partial r} r \frac{\partial}{\partial r} \delta\phi^l(r) - \frac{l^2}{r^2} \delta\phi^l(r) = -\frac{l}{r\omega_{ce}} \frac{\delta\phi^l(r)}{[\omega - l\omega_{re}]} \frac{\partial}{\partial r} \omega_{pe}^2(r). \quad (3)$$

Here ω_{ce} is the cyclotronic frequency, l is the azimuthal mode number, and ω_{re} and ω_{pe} are respectively the slow branch equilibrium azimuthal rotation frequency and equilibrium electron plasma frequency. ω is the complex frequency of the Diocotron mode and determines the stability. The boundary conditions are $\delta\phi^l(a) = 0$ and $\delta\phi^l(b) = 0$.

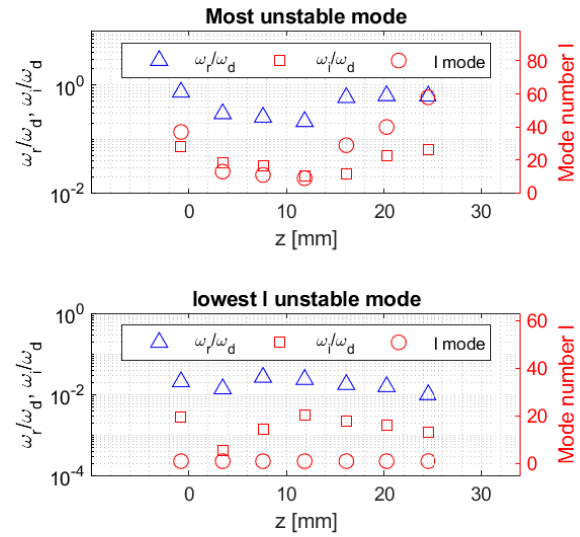


Figure 4: Top: most unstable mode complex frequency and mode number l for density profiles taken along the radial direction. Bottom: complex frequency and mode number l for the unstable mode with lowest l . The frequencies are normalized by $\omega_d = \max(\frac{2\omega_{pe}^2(r,z)}{\omega_{ce}(r,z)})$ the maximal local diocotron frequency.

In our PIC simulations, the steady-state density profile is axially non-uniform, thus we perform diocotron stability studies at different axial positions, effectively studying slices of the electron cloud. The results of this study, represented in figure 4, show that the steady state electron cloud is in fact diocotron unstable for several mode numbers l and that studying the stabilizing factors is necessary. For illustration, an unstable normal mode is represented in the (x,y) space in figure 5.

Conclusions and outlooks

With this study, we have shown that using an ad-hoc source, the system reaches a steady-state and no axial or radial instability has been observed. This steady state is strongly dependent on the magnetic field amplitude and to a lower extent on the externally imposed potential bias between the trapping electrodes. Even though 2D stability has been achieved, it has been shown that the cloud is expected to be azimuthally unstable and further study is necessary. As a future step, we plan to relax the low density assumption and study diocotron modes with finite k_z . Finally, the self-consistent electron-cloud build-up will need to be studied, by implementing electron-neutral collisions and ionization in the PIC code, as these phenomena could lead to different equilibria and dynamical regimes.

Acknowledgements

This work has been carried out within the framework of the EUROfusion Consortium and has received funding from the Euratom research and training programme 2014-2018 and 2019-2020 under grant agreement No 633053.

The views and opinions expressed herein do not necessarily reflect those of the European Commission.

This work was supported in part by the Swiss National Science Foundation.

References

- [1] Pagonakis I Gr, Piosczyk B, Zhang J, Illy S, Rzesnicki T, Hogge J-P, et al 2016 *Phys. Plasmas* **23** 023105.
- [2] Piosczyk B, et al 2004 *IEEE Trans. Plasma Sci.* **32** 853-60.
- [3] Plasma Physics via Computer Simulation. (CRC Press, 2018). doi:10.1201/9781315275048.
- [4] Höllig K, Reif U, Wipper J 2001 *SIAM J Numer Anal.* **39**(2) 442-62.
- [5] Levy R H 1965 *The Physics of Fluids* **8**(7) 1288-95.
- [6] Davidson RC. *Physics of Nonneutral Plasmas*, (Imperial College Press, World Scientific Publishing, 2001) Chapter 6 Sec. 6.3.

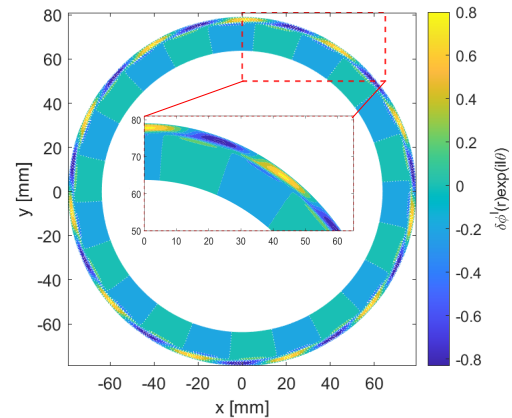


Figure 5: *Most unstable diocotron mode for radial the density profile taken at $z = 7.5\text{mm}$ in the steady state cloud of figure 2.*